

A Novel Prostate Segmentation Algorithm in TRUS Images

Ali Rafiee, Ahad Salimi, and Ali Reza Roosta

Abstract—Prostate cancer is one of the most frequent cancers in men and is a major cause of mortality in the most of countries. In many diagnostic and treatment procedures for prostate disease accurate detection of prostate boundaries in transrectal ultrasound (TRUS) images is required. This is a challenging and difficult task due to weak prostate boundaries, speckle noise and the short range of gray levels. In this paper a novel method for automatic prostate segmentation in TRUS images is presented. This method involves preprocessing (edge preserving noise reduction and smoothing) and prostate segmentation. The speckle reduction has been achieved by using stick filter and top-hat transform has been implemented for smoothing. A feed forward neural network and local binary pattern together have been use to find a point inside prostate object. Finally the boundary of prostate is extracted by the inside point and an active contour algorithm. A numbers of experiments are conducted to validate this method and results showed that this new algorithm extracted the prostate boundary with MSE less than 4.6% relative to boundary provided manually by physicians.

Keywords—Prostate segmentation, stick filter, neural network, active contour.

I. INTRODUCTION

PROSTATE cancer is the most frequently diagnosed cancer in men and the second cancer-related cause of death for this group [1],[2]. Hence diagnosis of the cancer in the early stages is crucial. Ultrasound imaging is a widely used technology for diagnosing and treatment this kind of cancer [1].

Prostate transrectal ultrasound (TRUS) images in comparison with the other modalities such as CT and MRI are captured easier, in real-time, and with lower cost. The accurate detection of the prostate boundary in ultrasound images is crucial for automatic cancer diagnosis/ classification and some clinical applications, such as the accurate placement of the needles during the biopsy, accurate prostate volume measurement from multiple frames, constructing anatomical models. However, Prostate region in TRUS prostate images maintains very weak texture structure. Because the low contrast, the fuzzy boundaries between the prostate and background, the speckle noise and shadow regions the

A. Rafiee is with Islamic Azad University-Kazeroun Branch, Kazeroun, Iran (phone: +98-917-1133925, fax: +98-721-2230508, e-mail: alirafiee_2000@yahoo.com).

A. Salimi is with Islamic Azad University-Najafabad Branch, Najafabad, Iran (e-mail: ahad.salimi@gmail.com).

A. R. Roosta is with Shiraz University of Technology, Shiraz, Iran (e-mail: Roosta@sutech.ac.ir).

ordinary analysis methods are not capable to segment the prostate region. In a typical TRUS screening, the prostate is manually delineated in the ultrasound image to calculate its size and volume, which are additional details used to support the diagnosis. The automated delineation of the prostate leads to faster, more accurate and precise results without much interference from the doctor [3]. Different methods of delineating the prostate, such as those presented in [3],[4], [5],[6] have shown to be successful in segmenting the prostate, however still requiring the input of the doctor to identify the prostate. Automated methods of TRUS prostate segmentation are in high demand and different segmentation methods have been proposed. Some methods have been introduced to investigate automatic or semi-automatic segmentation of the prostate such as region segmentation methods, boundary segmentation techniques, and deformable models [7], [8], [9], [10], [11], [12], [13], [14]. In this paper, we will investigate an algorithm of automatically identifying the prostate within the TRUS image. It consists of several sequential stages, include preprocessing, prostate inside point finding and segmentation. The preprocessing stages are stick filtering for speckle noise reduction and morphological smoothing. The prostate inside point finding is an adaptive and intelligent algorithm that finds a point in prostate region on TRUS images. This point is a critical point for prostate region detection which is the motivation for this work. The last stage is prostate segmentation base on the active contour model. This work is organized as follows: In section II the prostate segmentation system is described in detail. Section III validates the performance of the method via visual inspection and some quantitative measures. Section IV concludes the work.

II. PROSTATE SEGMENTATION SYSTEM

The segmentation system consists of 3 stages that are shown in Fig. 1. The first part is preprocessing, that includes stick filter and the morphological smoothing. The stick filter is used to reduce speckle noise with preserved edges information. The morphological smoothing includes two transformations, top-hat and bottom-hat [15],[16].

The second stage is the inside pixel finding that search any pixel in prostate region. This pixel is critical start point for segmentation. This stage includes 4 processes, the thresholds determine by the neural network system, the binarization of image by threshold, the labeling and the region investigation.

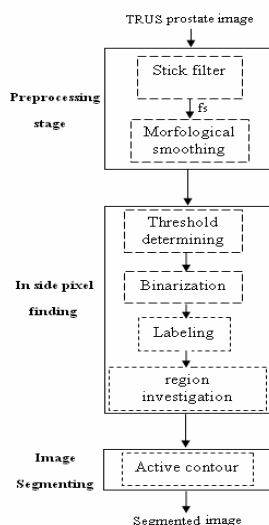


Fig. 1 The Segmentation system chart

A. Preprocessing

The study of adaptive low-pass filters has shown that these filters, although successfully filter much of the speckle, cause a loss of detail in low-contrast border regions [16]. An alternative method uses sticks to reduce speckle noise that it's named as a stick filter. The sticks filtering algorithm challenges the problem of filtering speckle in ultrasound images, without losing edge detail. The stick filter determine the mean of neighboring pixels in the direction of the stick - the most likely direction of the linear feature passing through (x,y). Assuming n is the stick's length in pixels, there are $2*n-2$ possible orientations of its can be arranged. A typical sticks of length five pixels, is shown in Fig. 2. In this figure the white and black pixels have a value of 0 and 1/5, respectively. Results showed that the stick filter increased the contrast near the prostate borders, and reduced speckle noise (Fig. 3).

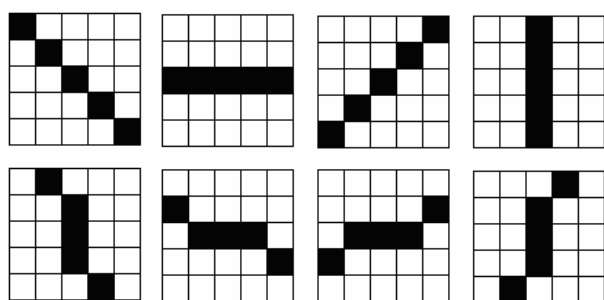


Fig. 2 A typical stick of length five pixels

The morphological algorithm is used to smooth filtered image and enhanced contrast near edges. The top-hat and bottom transformation apply on output of stick filter (F_s) with using a ordinary neighborhood window. In this work we use a disk with radius 3 in size in top-hat, bottom-hat transformations. The following equations have shown these transformations:

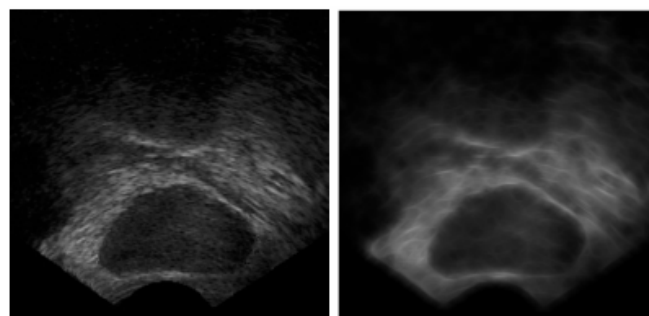


Fig. 3 The original TRUS image(left), output of stick filter(right)

$$H_t = top - hat(F_s) \quad (1)$$

$$H_b = bot - hat(F_s) \quad (2)$$

The top-hat and bottom-hat transformations of filtered images are used to increase the contrast, according to the following equation

$$F_p = F_s + H_t - H_b \quad (3)$$

H_t is the top-hat and H_b is the bottom-hat transformations and F_p is the preprocessed image. Fig. 4 has showed the morphological output of the prostate image.

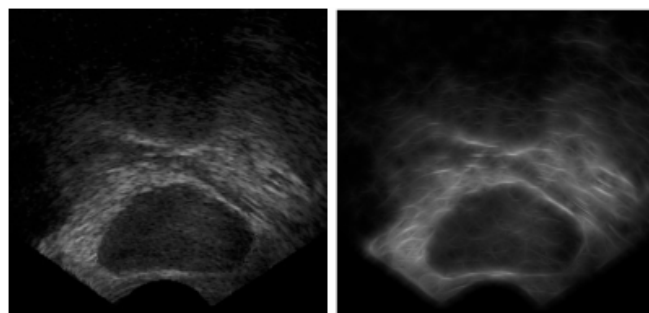


Fig. 4 The original Trus image (left), the output of morphological filter

B. Inside Pixel Finding

The inside pixel finding stage is the size and shape independent algorithm that uses the neural network, binarization, labeling and prostate region investigation. The neural network is used to find the prostate region grey level thresholds. The prostate region thresholds are the critical values that are used to binarization images. A feed forward neural network is used to find the optimum values for the high and low grey level thresholds. The NN is 3 layers network and train by back propagation learning algorithm (Fig. 5). The inputs for NN are the column averages of the central region of TRUS preprocessed images. The size of this region is about 200columns. The output of NN is 2 threshold values.

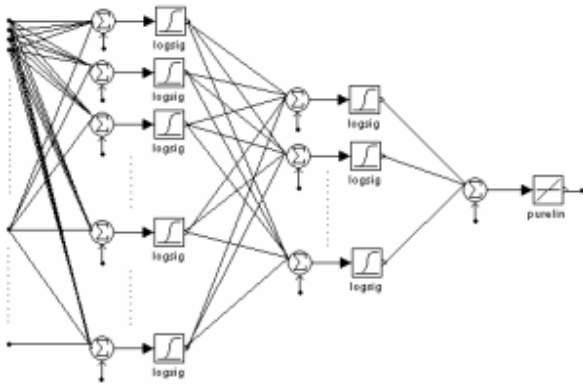


Fig. 5 A 3-layer NN for estimate threshold value

These values are used to labeled image pixels as a binary class. A typical neighborhood window of each pixel is considered to be multiplied by its weights to evaluate the central pixel. In the window each pixel that is between the high and low threshold take 1 and the others take 0 as it can be seen in Fig. 6. The following relation is showed the binarization process of the image pixels:

$$P_i^0 = \sum_{j=1}^8 T_i^j * W_i^j \quad (4)$$

$$T_i^j = \begin{cases} 1 & \text{if } P_i^j \in [T_{low}, T_{high}] \\ 0 & \text{otherwise} \end{cases} \quad (5)$$

T_{low} is the low threshold, T_{high} is the high threshold, W_i^j is the pixel weight (as showed in Fig. 6) and P_i^j is the j th pixel in neighborhood window and P_i^0 is the central pixel. The binarized image is used to label and classified the distinct regions.

W_i^1	W_i^2	W_i^3
W_i^8		W_i^4
W_i^7	W_i^6	W_i^5

1	2	4
128		8
64	32	16

Fig. 6 Neighborhood window and associated weights for binarization

Then the region with the most area is selected as a first estimation of prostate region (Fig. 7). The central pixel in this region is selected as a start point for active contour segmentation algorithm.



Fig. 7 Binarization the image(left), select the most area region(middle), inside point finding(right)

C. Active Contour Model Segmentation

The active contour model algorithm deforms a contour to look onto features of interest within in an image [17]. Usually the features are lines, edges, and/or object boundaries. Active contour models should be able to find the prostate boundary in TRUS images. An active contour is an ordered collection of n points in the TRUS image that iteratively approach the boundary of an object through the solution of an energy minimization problem. The energy function is in two terms, the internal and external energies. The internal energy depends on the shape of contour and the external energy depends on image properties such as gradient. An active contour is set of n points in the image and energy for each point is defined as follow:

$$C = \{c_1, c_2, c_3, \dots, c_n\} \quad (6)$$

$$E(c_i) = \alpha E_{int}(c_i) + \beta E_{ext}(c_i) \quad (7)$$

E , E_{int} and E_{ext} are matrices that the value at the center of each matrix corresponds to the contour energy at point c_i . Other values in the matrices correspond (spatially) to the energy at each point in the neighborhood of c_i . Each point, c_i , is moved to the point, c_i' , corresponding to the location of the minimum value in E . The contour, C , should approach, and stop at, the region boundary.

The internal energy itself, contain two terms elastic and bending energy that has shown as follow:

$$E_{int}(c_i) = E_{elastic}(c_i) + E_{bending}(c_i) \quad (8)$$

Where $E_{elastic}$ is the elastic energy that enforces the shape of the contour and $E_{bending}$ is a bending force that causes the contour to grow balloon or shrink. The formulation of the elastic energy is defined as follows:

$$e_{jk}(c_i) = \frac{1}{N(c)} \left\| p_{jk}(c_i) - (c_{i-1} + c_{i+1}) \right\|^2 \quad (9)$$

Where p_{jk} is the point in the image that corresponds spatially to energy matrix element e_{jk} .

The normalization factor, N , is the average distance between points in contour:

$$N(c) = \frac{1}{n} \sum_{i=1}^n \|c_{i+1} - c_i\|^2 \quad (10)$$

The normalization is required to make E_{elastic} independent of the size, location, and orientation of contour.

A bending force can be used on a closed deformable contour to force the contour to expand in the absence of external influences. A contour initialized within a uniform image object will expand under the influence of a bending force until it nears the region boundary the energy term for each element, b_{jk} , in the matrix, E_{bending} is expressed as a dot product:

$$b_{jk}(c_i) = v_i \cdot (c_i - p_{jk}(c_i)) \quad (11)$$

Where v_i is the outward unit normal of C at point c_i . Therefore, the bending energy is smallest at points farthest from c_i in the direction of v_i .

The external energy function attracts the deformable contour to interesting features, such as region boundaries. Image gradient and intensity are obvious features to look at for external energy. Therefore, the following external energy function is investigated:

$$E_{\text{ext}}(c_i) = E_{\text{intens}}(c_i) + E_{\text{grad}}(c_i) \quad (12)$$

Where E_{intens} is an expression that attracts the contour to high or low intensity regions and E_{grad} is an energy term that moves the contour towards edges. Each element in the intensity energy matrix is assigned the intensity value of the corresponding image point in the neighborhood of c_i . The image gradient energy function is proportional to the gradient magnitude. When active contours are used to find region boundaries, an energy expression that discriminates between edges of adjacent region is desirable. The key to such an expression is that the gradients at the edges of the region have different directions. Further, the direction of the gradient at the region edge should be similar to the direction of the unit normal of the contour.

III. RESULTS

The first step is noise reduction by applying stick filter. Table I showed the mean square error results of stick filter with various sizes in stick. As showed in Table I the best size of stick for speckle reduction in TRUS images is 5. For inside pixel finding a NN with 2 homogenous sub networks is used. In each sub network, 3 layers are used. The input layer had 100 neurons, the hidden layers are 10 neurons layer and the output layer is 1 neuron. For NN training the half of images in database (that are 50 TRUS images of prostate) is used randomly. The others are used for algorithm testing. The NN is trained after 250000 epoches and the optimum values for threshold are determined. In all test images the inside point has found correctly.

TABLE I
 MSE OF NOISE REDUCTION STICK FILTER
 VERSUS STICK LENGTH AND THICKNESS

STICK'S LENGHT	STICK'S THICKNESS	MSE
5	1	0.046
5	3	0.130
7	1	0.072
9	1	0.095
15	1	0.150

The active contour model algorithm has been implemented on TRUS images and the boundary of prostate is specified. For comparison the initial contour provided by the specialist of sonography images has also considered. The mean square error of the areas between the output of algorithm and the boundary extracted by the sonographer is used for evaluation of algorithm performance. Fig. 8 shows the comparison of the algorithm result and the boundary provided by sonographer idea. The mean square error for all images is less than 4.6%.

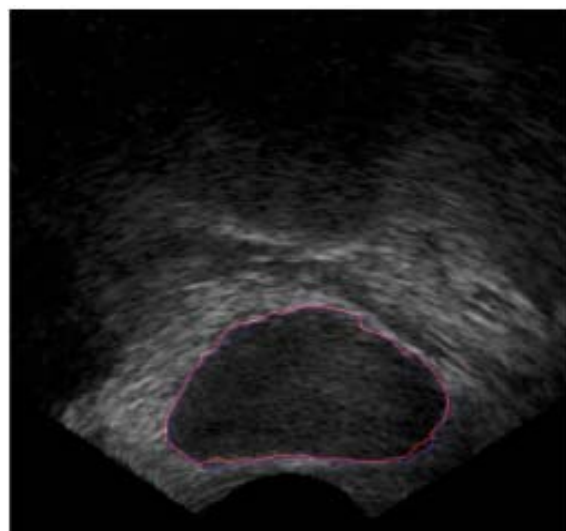


Fig. 8 Comparison of boundaries provided by segmentation system (blue) and the sonographer (red)

IV. CONCLUSION

In this study we have used a new algorithm for prostate segmentation in TRUS images. This algorithm also reduces speckle noise and enhanced the edge contrast. Results showed that the segmented objects are very similar to objects that provided manually by physician.

REFERENCES

- [1] Cancer Facts and Figures. American Cancer Society. [Online] <http://www.cancer.org>, 2002.
- [2] Mettlin C: American society national cancer detection project. Cancer 1995, 75:1790-1794.
- [3] Sayan D. Pathak, Vikram Chalana, David R. Haynor, and Yongmin Kim. Edge-guided boundary delineation in prostate ultrasound images. IEEE Trans. Med. Imaging, 19(12):1211-1219, 2000.

- [4] J. M. Fitzpatrick and J. M. Reinhardt, editors. Prostate ultrasound image segmentation using level set-based region flow with shape guidance. SPIE, Apr. 2005.
- [5] Ahmed Jendoubi, Jianchao Zeng, and Mohamed F. Chouikha. Top-down approach to segmentation of prostate boundaries in ultrasound images. In AIPR, pages 145-149, 2004.
- [6] Farhang Sahba, Hamid R. Tizhoosh, and Magdy M.A. Salama. Segmentation of prostate boundaries using regional contrast enhancement. In the IEEE International Conference on Image Processing (ICIP), volume 2, pages 1266-1269, Sept. 2005.
- [7] C.K. Kwok, M. Teo, W. Ng, S. Tan, and M. Jones "Outlining the prostate boundary using the harmonics method," Med. Biol. Eng. Computing, vol. 36, pp. 768-771, 1998.
- [8] R.G. Aarnink, R.J.B. Giesen, A. L. Huynen, J. J. de la Rosette, F.M. Debruyne, and H. Wijkstra, "A practical clinical method for contour determination in ultrasound prostate images," Ultrasound Med. Biol., vol. 20, pp. 705-717, 1994.
- [9] R.G. Aarnink, S.D. Pathak, J. J. de la Rosette, F.M. Debruyne, Y. Kim and H. Wijkstra, "Edge detection in ultrasound prostate images using integrated edge map.," Ultrasound Med. Biol., vol. 36, pp. 635-642, 1998.
- [10] Y. Zhan and D. Shen, "Deformable segmentation of 3-d ultrasound prostate images using statistical texture matching method," IEEE Transactions on Medical Imaging, vol. 25, pp. 256-272, 2006.
- [11] D. Freedman, R.J. Radke, T. Zhang, Y. Jeong, D.M. Lovelock, and G.T.Y. Chen, "Model-based segmentation of medical imagery by matching distributions," IEEE Transactions on Medical Imaging, vol. 24, pp. 281-292, 2005.
- [12] A. Ghanei, H. Soltanian-Zadeh, A. Ratkewicz, and F. Yin, "A three dimensional deformable model for segmentation of human prostate from ultrasound images," Med. Phys, vol. 28, pp. 2147-2153, 2001.
- [13] C. Knoll, M. Alcaniz, V. Grau, C. Monserrat, and M. Juan, "Outlining of the prostate using snakes with shape restrictions based on the wavelet transform," Pattern Recognition, vol. 32, pp. 1767-1781, 1999.
- [14] S. D. Pathak, V. Chalana, D. haynor, and Y. kim, "Edge guided boundary delineation in prostate ultrasound images," IEEE Transactions on Medical Imaging, vol. 19, pp. 1211-1219, 2000.
- [15] R.C. Gonzalez and R.E. Woods. Digital Image Processing, 2nd. Ed. Prentice-Hall, 2002.
- [16] R.C. Gonzalez and R.E. Woods. Digital Image Processing using matlab. Ed. Prentice-Hall, 2004.
- [17] Michael Kass, Andrew Witkin, and Demetri Terzopoulos. Snakes: Active contour models. International Journal of Computer Vision, pages 321-331, 1988.